Available online at www.sciencedirect.com
SCIENCE DIRECT
Chemical Physics Letters 422 (2006) 475–480
CHEMICAL PHYSICS LETTERS
www.elsevier.com/locate/cplett

Dissociation of energy-selected c-$C_3H_6S^+$ studied with threshold photoelectron-photoion coincidence experiments and calculations

Su-Yu Chiang [a,*], Yung-Sheng Fang [b], Chun-Neng Lin [b]

[a] National Synchrotron Radiation Research Center, Research Division, 101, Hsin Ann Road, Hsinchu Science Park, Hsinchu 30076, Taiwan
[b] Department of Applied Chemistry, National Chiao Tung University, 1001, Ta Hsueh Road, Hsinchu 30010, Taiwan

Received 24 November 2005; in final form 6 March 2006
Available online 10 March 2006

Abstract

The dissociation of energy-selected c-$C_3H_6S^+$ was investigated in a region 10.2–10.9 eV with a threshold photoelectron-photoion coincidence technique. Branching ratios and average releases of kinetic energy for channel c-$C_3H_6S^+ \rightarrow H_2CS^+ + C_2H_4$ were derived from coincidence mass spectra. The measured small releases of kinetic energy near the appearance onset agree with statistical calculations; a linearly extrapolated threshold at 10.39 ± 0.01 eV agrees with a predicted energy 10.35 eV with the GAUSSIAN-3 method. We discuss plausible mechanisms for c-$C_3H_6S^+$ dissociating to $CH_3CS^+ + CH_3$ based on G3B3 calculations to rationalize the absence of CH_3CS^+ signal in these experiments.
© 2006 Elsevier B.V. All rights reserved.

1. Introduction

The four-membered ring molecule thietane (c-C_3H_6S) has been the subject of numerous spectral investigations and theoretical calculations as a result of efforts to understand the vibrational effects on the ring structure: ring-puckering motions likely alter the planar structure enforced by ring strain [1,2]. The photochemistry of c-C_3H_6S is also of fundamental importance as photodissociation or photoionization of c-C_3H_6S offers a powerful means to produce reactive H_2CS or H_2CS^+ that plays an important role in atmospheric chemistry and serves as a prototypical system in the chemistry of sulfur-containing organic compounds [3–12].

Several groups reported that photodissociation of c-C_3H_6S yields exclusively $H_2CS + C_2H_4$ on excitation at 313 and 254 nm; based on experimental results, those authors proposed that dissociation proceeds through a direct breaking of the C–S bond to form a diradical, with subsequent rearrangement [3–5]. The channel $S + C_3H_6$ was also observed on excitation at 214 and 193 nm; ground-state $S(^3P)$ atoms are predominantly produced at 214 nm, but excited $S(^1D)$ atoms are formed exclusively at 193 nm [6–8]. With photon energy of excitation increasing into the vacuum ultraviolet (VUV) region, dissociative photoionization of c-C_3H_6S takes place; the dissociation of c-$C_3H_6S^+$ is expected to become more complicated, as isomerization and rearrangement of ionized polyatomic molecules commonly occur before dissociation [9–11].

Butler and Baer investigated the dissociative photoionization of c-C_3H_6S in a region 8.5–13.5 eV with photoionization mass spectroscopy (PIMS); four fragment ions – H_2CS^+, $C_2H_3S^+$, HCS^+, and $C_3H_5^+$ – were identified with their respective appearance energies (AE) 9.9, 10.0, 10.4, and 10.5 eV at 298 K, determined from the onsets of photoionization efficiency (PIE) curves [9,10]. According to these determined AE, heats of formation of H_2CS^+, $C_2H_3S^+$ and HCS^+ were derived, but such AE values represent upper limits due to the possible presence of exit channel barriers and kinetic shifts [13,14]. In the present work, we pursue our investigation

* Corresponding author. Fax: +886 3 578 3813.
E-mail address: schiang@nsrrc.org.tw (S.-Y. Chiang).

0009-2614/$ - see front matter © 2006 Elsevier B.V. All rights reserved.
doi:10.1016/j.cplett.2006.03.020

of the dissociation of energy-selected c-$C_3H_6S^+$ in a region 10.2–10.9 eV with a threshold photoelectron-photoion coincidence (TPEPICO) technique to obtain branching ratios and average releases of kinetic energy for channel $H_2CS^+ + C_2H_4$. We also predict plausible dissociation mechanisms for channel c-$C_3H_6S^+ \rightarrow CH_3CS^+ + CH_3$ with the G3B3 method to shed light on the lack of observation of CH_3CS^+ in this energy region.

2. Experiments

The coincidence measurements were conducted on the Seya-Namioka beamline at the NSRRC in Taiwan. Photon energies with resolution 30 meV and photon flux $>10^9$ photons s^{-1} in a region 10.2–10.9 eV were selected with a monochromator (1 m; 1200 grooves mm^{-1}; slit width 0.15 mm). Absolute photon energies were calibrated within ±0.006 eV on measurement of Rydberg signals in the threshold photoelectron spectrum of Ar.

The molecular beam/threshold photoelectron photoion coincidence (MB/TPEPICO) system is described in detail elsewhere [15,16]. Briefly, a mixture of c-C_3H_6S (Aldrich, ~98%) and He (>99.999%) at a total stagnation pressure ~280 Torr and with a seed ratio ~10% was expanded through a nozzle and two skimmers to form a cooled c-C_3H_6S beam to be ionized in the ionization chamber. The threshold electrons produced were extracted with a dc field 100 V m^{-1} and analyzed with a threshold photoelectron spectrometer; the ions produced were extracted with an electric field 2100 V m^{-1} with pulses of duration 30 μs on detecting a threshold electron and analyzed with a time-of-flight mass spectrometer. A time-to-digital converter (TDC) was used to record the flight durations of ions that were triggered with a threshold electron and a signal generated randomly relative to the preceding threshold electron signal. Subtraction of the randomly generated coincidence spectrum from the electron-triggered coincidence spectrum yielded a true coincidence spectrum. All data acquisition was controlled with a computer via a CAMAC interface and the output of TDC was transferred to a computer for further processing.

3. Calculations

All molecular structures and energies of c-C_3H_6S and species pertinent to this work were calculated using the GAUSSIAN 2003 program [17]. For calculations of G3 energy,E_0(G3), the equilibrium structure was fully optimized at the MP2(full)/6-31G(d) level, and single-point calculations were performed at levels MP4/6-31G(d), QCISD(T)/6-31G(d), MP4/6-31+G(d), MP4/6-31G(2df,p), and MP2(full)/G3large; additional energies include a spin-orbit correction, higher-level corrections and a zero-point vibrational energy (ZPVE) calculated from the HF/6-31G(d) vibrational frequencies on scaling by 0.8929. For a comparison, we also calculated G3 energies, E_0(G3-B), using B3LYP/6-31G(d) vibrational frequencies with a scaling factor 0.9613 for ZPVE correction and calculated G3B3 energies, E_0(G3B3), with single-point calculations performed at an equilibrium structure fully optimized at the B3LYP/6-31G(d) level. Transition structures were located with geometries optimized at the B3LYP/6-31G(d) level because some dissociation paths could not be confirmed with intrinsic reaction coordinate (IRC) calculations at the MP2(full)/6-31G(d) level; all identified transition structures were verified to have only one imaginary vibrational frequency.

4. Results and discussion

4.1. Coincidence mass spectra in a region 10.2–10.9 eV

The threshold photoelectron (TPE) spectrum of c-C_3H_6S measured with an energy step ~0.01 eV in a region 8.5–11.5 eV agrees with the photoelectron (PE) spectrum [18]. One broad band observed in a region ~10.05 to 11.63 eV with maximum at ~10.59 eV corresponds to the removal of a $10a_1$ (σ_{C-S}) electron; dissociation of energy-selected c-$C_3H_6S^+$ associated with excitation to this ionic excited state was investigated in this work.

The coincidence mass spectra of c-C_3H_6S were recorded at selected photon energies in a region 10.2–10.9 eV. Fig. 1a–e show corrected coincidence mass spectra of

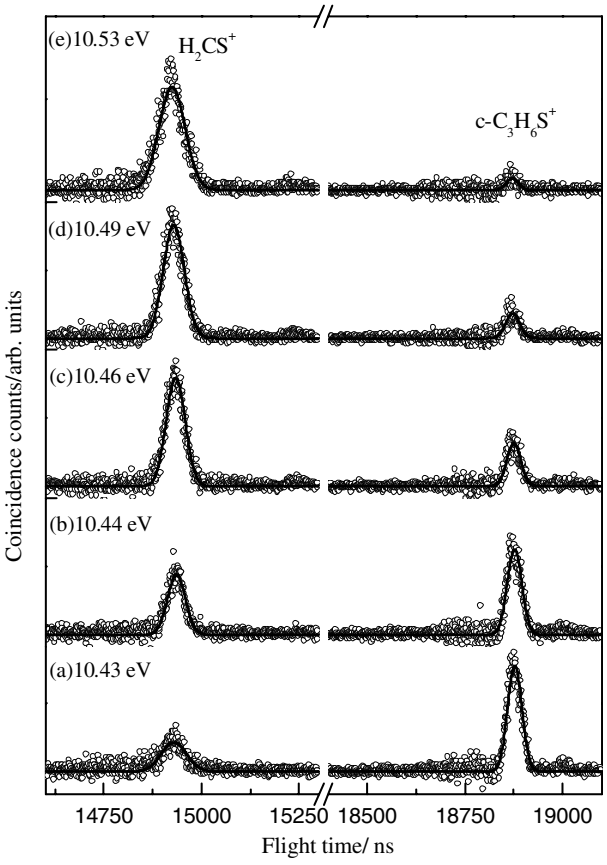

Fig. 1. Coincidence mass spectra of c-C_3H_6S excited at photon energies (a) 10.43 eV (b) 10.44 eV (c) 10.46 eV (d) 10.49 eV and (e) 10.53 eV.

c-C_3H_6S excited at 10.43, 10.44, 10.46, 10.49 and 10.53 eV; solid lines indicate ion time-of-flight (TOF) signals fitted to Gaussian shapes, and all spectra are normalized to 5000 total electron triggers. Ion signals at $m/z = 74$ and 46, corresponding to c-$C_3H_6S^+$ and H_2CS^+, respectively, were identified according to ion flight durations calculated with an equation $T_0/\text{ns} = 2161.8\ (m/z)^{1/2} + 248$ obtained from coincidence mass spectra of He, Ar and Kr.

In the figures, TOF signals of c-$C_3H_6S^+$ fitted to a Gaussian profile have a full width at half maximum (fwhm) ~42 ns; the transverse temperature of the molecular beam is accordingly calculated to be 22 K [19]. TOF signals of H_2CS^+ were also fitted well to a Gaussian profile, but the bandwidth of TOF signals increases with increasing photon energy, reflecting releases of kinetic energy upon dissociation. Obtained fwhm of TOF signals of H_2CS^+ and calculated average releases of kinetic energy for channel c-$C_3H_6S^+ \rightarrow H_2CS^+ + C_2H_4$ are listed in Table 1. Average release of kinetic energy, ⟨KE⟩, was calculated from fwhm according to the Maxwellian equation [19,20]

$$\langle \text{KE} \rangle = \frac{3}{16 \ln 2} (e\varepsilon)^2 (\text{fwhm})^2 \frac{M_\text{p}}{M_\text{f}(M_\text{p} - M_\text{f})} - \frac{3}{2} RT \times \frac{M_\text{f}}{(M_\text{p} - M_\text{f})} \quad (1)$$

in which $e = 1.602 \times 10^{-19}$ C is the charge, $\varepsilon = 2100$ V m^{-1} is the strength of the pulsed electric field for ion extraction, M_p and M_f are masses of c-$C_3H_6S^+$ and H_2CS^+, and $T = 22$ K is the transverse temperature of the molecular beam.

4.2. Branching ratios and average releases of kinetic energy

Fig. 2 shows the branching ratios of c-$C_3H_6S^+$ and fragment ion H_2CS^+ in a region 10.2–10.9 eV obtained from the area ratios of their TOF signals in coincidence mass spectra. H_2CS^+ appears in a region 10.39–10.41 eV; a cross at 10.44 eV reflects that half of c-$C_3H_6S^+$ ions dissociate to form H_2CS^+ at that energy. Formation of H_2CS^+ is likely attributable to increased internal energy of c-$C_3H_6S^+$ as the dissociation threshold 10.39–10.41 eV lies above the onset at ~10.20 eV of the excited state of c-$C_3H_6S^+$ observed in our TPE spectrum and a previous PE spectrum [18]. Table 2 lists calculated G3 energies – E_0(G3) and E_0(G3B3) – for species pertinent to dissociative photoionization of c-C_3H_6S, and energy differences – ΔE(G3) and ΔE(G3B3) – relative to c-$C_3H_6S^+$; E_0(G3-B) and ΔE(G3-B) are not listed due to small differences between ΔE(G3B3) and ΔE(G3-B). A predicted G3 energy 10.35 eV for dissociative photoionization of c-C_3H_6S to form $H_2CS^+ + C_2H_4$ agrees with an observation of a dissociation threshold 10.39–10.41 eV.

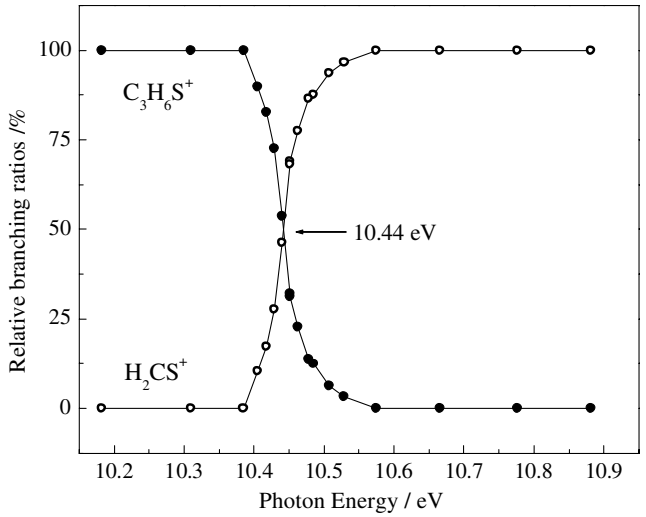

Fig. 2. Branching ratios of c-$C_3H_6S^+$ and H_2CS^+ in a region 10.2–10.9 eV; fractional abundances of these two ions were obtained from their total TOF signals.

Fig. 3 shows the calculated average releases of kinetic energy for channel c-$C_3H_6S^+ \rightarrow H_2CS^+ + C_2H_4$; a solid line indicates a linear fit to data near the dissociation threshold and a dashed curve results from QET calculations, performed according to an equation formulated by Klots [21–23]

$$h\nu - E_0 = \frac{(r+1)}{2} \langle \text{KE} \rangle + \sum_i \frac{h\nu_i}{\exp\left(\frac{h\nu_i}{\langle \text{KE} \rangle}\right) - 1} \quad (2)$$

in which $h\nu$ is the photon energy, $E_0 = 10.39 \pm 0.01$ eV is the linearly extrapolated dissociation threshold, r is the number of rotational degrees of freedom and ν_i are vibrational wave numbers of H_2CS^+ and C_2H_4; the latter values are 3038, 2929, 1382, 962, 935 and 830 cm^{-1} for H_2CS^+ and 2988, 1656, 1336, 1031, 2967, 1437, 981, 3056, 800, 3033, 1207 and 977 cm^{-1} for C_2H_4, obtained from the HF/6-31G(d) calculations.

A dissociation threshold at 10.39 ± 0.01 eV obtained by linearly extrapolating data at photon energies smaller than 10.6 eV agrees with a G3 prediction 10.35 eV. Also seen in Fig. 3, QET calculations with a dissociation threshold at 10.39 ± 0.01 eV fit satisfactorily the experimental data near the dissociation threshold. The agreements on dissociation threshold and a statistical distribution of ⟨KE⟩ near threshold imply that c-$C_3H_6S^+$ dissociates to $H_2CS^+ + C_2H_4$ without significant exit channel barrier. Moreover, a statistical

Table 1
Calculated average releases of kinetic energy (⟨KE⟩) from the full width at half maximum (fwhm) for channel c-$C_3H_6S^+ \rightarrow H_2CS^+ + C_2H_4$

PE (eV)	fwhm (ns)	⟨KE⟩ (eV)
10.88	111	0.076
10.78	105	0.068
10.67	95	0.055
10.57	88	0.047
10.53	79	0.036
10.51	71	0.028
10.49	64	0.022
10.46	58	0.017
10.45	51	0.013
10.44	54	0.015
10.43	50	0.012

Table 2
Calculated G3 energies, E_0(G3) and E_0(G3B3), for species pertinent to dissociative photoionization of c-C_3H_6S, and energy differences, ΔE(G3) and ΔE(G3B3), relative to c-$C_3H_6S^+$

Species	Sym.	E_0(G3) (hartree)	E_0(G3B3) (hartree)	ΔE(G3) (eV)	ΔE(G3B3) (eV)
c-C_3H_6S	C_s	−515.82967	−515.83323	−8.68	−8.67
c-$C_3H_6S^+$	C_s	−515.51058	−515.51474	0.00	0.00
$CH_2CH_2SCH_2^+$ (1+)	C_s	−515.48267		0.76	
cis-$CH_3CHSCH_2^+$ (2+)	C_s	−515.50562	−515.50855	0.13	0.17
trans-$CH_3CHSCH_2^+$ (3+)	C_s	−515.50632	−515.50930	0.12	0.15
cis-$CH_3CSCH_3^+$ (4+)	C_s	−515.48718	−515.49115	0.64	0.64
trans-$CH_3CSCH_3^+$ (4′+)	C_s	−515.48937	−515.49290	0.58	0.59
$CH_2CHSCH_3^+$ (5+)	C_s	−515.52267	−515.52565	−0.33	−0.30
TS1	C_1	−515.45757	−515.46128	1.44	1.45
TS2	C_1		−515.45048		1.75
TS3	C_1		−515.48706		0.75
TS4	C_1	−515.43070	−515.43420	2.17	2.19
TS5	C_1	−515.45949	−515.46277	1.39	1.41
TS6	C_1	−515.44007	−515.44349	1.92	1.94
C_2H_4	D_{2h}	−78.50741	−78.50930		
H_2CS^+	C_{2v}	−436.94173	−436.94368		
CH_3	D_{3h}	−39.79329	−39.79362		
CH_3CS^+	C_{3v}	−475.67411	−475.67700		
CH_2CSH^+	C_s	−475.63377	−475.63672		
c-$C_2H_3S^+$	C_s	−475.62884	−475.63155		
HCS^+	$C_{\infty v}$	−436.36196	−436.36414		
C_2H_5	C_s	−79.06398	−79.06569		
$C_3H_5^+$	C_{2v}	−116.84411	−116.84657		
HS	$C_{\infty v}$	−398.59531	−398.59664		

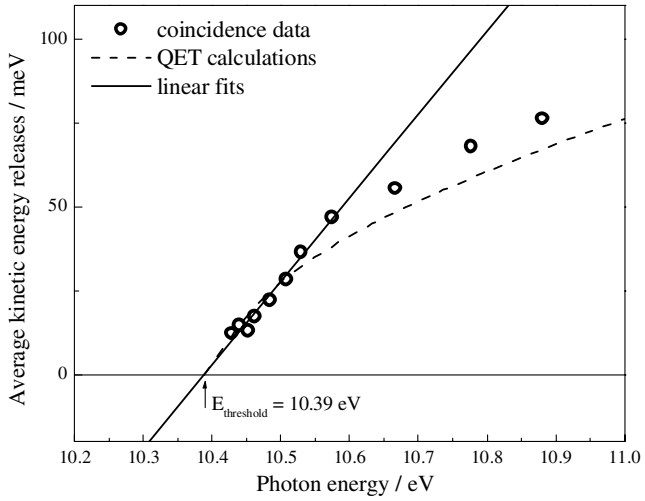

Fig. 3. Average kinetic energies released in the channel c-$C_3H_6S^+ \rightarrow H_2CS^+ + C_2H_4$ with excitation at photon energies in a region 10.4–10.9 eV.

interpretation of the variation of ⟨KE⟩ with photon energy cannot be valid if unimolecular dissociation occurs from the four-membered ring parent ion; isomerization and cleavage of the C–S bond will, however, give the predicted linear variation near threshold. Lee et al. predicted $CH_2CH_2SCH_2^+$ (1+) to be less stable than c-$C_3H_6S^+$ by 0.80 eV with the G3 method and located a transition state connecting $CH_2CH_2SCH_2^+$ (1+) to c-$C_3H_6S^+$ with a G3 barrier at 0.64 eV; they also predicted a dissociation energy 0.93 eV for channel $CH_2CH_2SCH_2^+$ (1+) → $H_2CS^+ + C_2H_4$, but located no transition state for this dissociation [24,25]. Accordingly, a dissociation mechanism that c-$C_3H_6S^+$ isomerizes to $CH_2CH_2SCH_2^+$ (1+) before dissociating to $H_2CS^+ + C_2H_4$ supports our experimental observation.

4.3. Theoretical predictions

We detected none of the three fragment ions – $C_2H_3S^+$, HCS^+ and $C_3H_5^+$ – identified in a previous PIMS experiment in a region 10.2–10.9 eV [9]. The absence of HCS^+ signal in this region is consistent with our G3 prediction of 10.99 eV for formation of $HCS^+ + C_2H_5$. The AE of 10.5 eV at 0 K for HCS^+ in the PIMS experiment is underestimated according to our G3 prediction and that the resultant $\Delta H^\circ_{f,0}(HCS^+) = 233 \pm 2$ kcal mol^{-1} derived from the AE of 10.5 eV is smaller than the established experimental values of 243.9 and 243.5 ± 2 kcal mol^{-1} [12,26]. The AE of 10.6 eV at 0 K for $C_3H_5^+$ in the PIMS experiment agrees coincidentally with our G3 prediction of 10.62 eV for formation of $C_3H_5^+ + HS$ despite the possible presence of kinetic shifts and activation barriers. Moreover, as the AE of 10.0 eV at 0 K for H_2CS^+ in the PIMS experiment is also significantly smaller than our G3 prediction of 10.35 eV and the linearly extrapolated threshold at 10.39 ± 0.01 eV, an underestimation of the AE values for $C_3H_5^+$ and $C_2H_3S^+$ in the PIMS experiment could be possible; discussion on the absence of these two ions in this work based on the PIMS results is thus discarded.

The predicted G3 energies for formation of $CH_3CS^+ + CH_3$, $CH_2CSH^+ + CH_3$, c-$C_2H_3S^+ + CH_3$ are 9.86, 10.96 and 11.09 eV, respectively; formation of $CH_3CS^+ + CH_3$

is the most likely channel on energetic grounds and requires the least energy relative to 10.35 eV for formation of $H_2CS^+ + C_2H_4$. If this is the case, the absence of CH_3CS^+ signal in this work indicates that greater activation energies during dissociation are applicable for H migrations and structural alterations. We explored dissociation mechanisms for channel c-$C_3H_6S^+ \rightarrow CH_3CS^+ + CH_3$ with the G3B3 method.

Fig. 4a,b show relative energies ΔE(G3B3) of two feasible dissociation mechanisms except ΔE(G3-B) for $CH_2CH_2SCH_2^+$ (1+) due to the failure of G3B3 calculations at the QCISD(T)/6-31G(d) level. Relative energies ΔE(G3) are not adopted in the figure because reaction paths for TS2 and TS5 optimized at the MP2(full)/6-31G(d) level could not be confirmed with IRC calculations. Nevertheless, according to Table 2, the difference between ΔE(G3B3) and ΔE(G3) is only 0.04 eV despite ΔE(G3B3) greater than ΔE(G3). In Fig. 4a, c-$C_3H_6S^+$ first breaks the C–C bond via TS1 to form intermediate $CH_2CH_2SCH_2^+$ (1+) with a G3B3 barrier at 1.45 eV. Next, $CH_2CH_2SCH_2^+$ (1+) undergoes H migration from the central CH_2 group to the terminal CH_2 group via TS2 with a barrier at 1.75 eV to form intermediate $CH_3CHSCH_2^+$ (2+). Finally, *cis*-$CH_3CHSCH_2^+$ (2+) rotates dihedral angle ∠CCSC via TS3 with a barrier at 0.75 eV to form *trans*-$CH_3CHSCH_2^+$ (3+), which subsequently proceeds through H migration via a four-membered ring TS4 with a barrier at 2.19 eV to form a dissociation precursor *trans*-$CH_3CSCH_3^+$ (4′+). The other dissociation precursor *cis*-$CH_3CSCH_3^+$ (4+) might be formed from intermediate *cis*-$CH_3CHSCH_2^+$ (2+). In Fig. 4b, *cis*-$CH_3CHSCH_2^+$ (2+) proceeds through H migrations from the CH_3 group to the CH_2 group and from the CH group to the CH_2 group via TS5 and TS6 with their predicted barriers at 1.41 and 1.94 eV, respectively, to form a

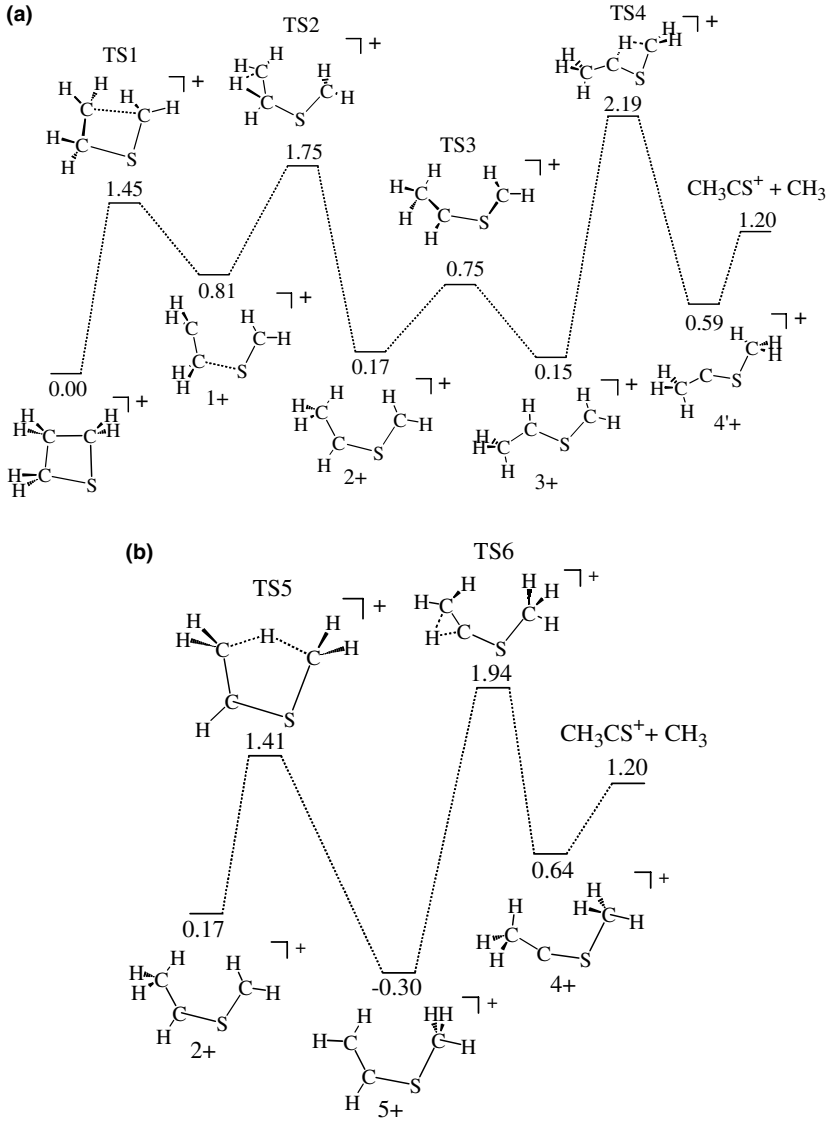

Fig. 4. Theoretical predictions of relative energies ΔE(G3B3) of two feasible dissociation mechanisms for channel c-$C_3H_6S^+ \rightarrow CH_3CS^+ + CH_3$ (a) isomerization of c-$C_3H_6S^+$ into *trans*-$CH_3CSCH_3^+$ (4′+) (b) isomerization of *cis*-$CH_3CHSCH_2^+$ (2+) into *cis*-$CH_3CSCH_3^+$ (4+).

more stable isomer $CH_2CHSCH_3^+$ (5+) and a dissociation precursor *cis*-$CH_3CSCH_3^+$ (4+). Finally, a direct cleavage of the C–S bond in *trans*-$CH_3CSCH_3^+$ (4′+) or in *cis*-$CH_3CSCH_3^+$ (4+) to form $CH_3CS^+ + CH_3$ requires no exit barrier.

Experimentally, we observed no CH_3CS^+ signal in a region 10.2–10.9 eV. c-C_3H_6S excited at 10.2–10.9 eV corresponds to 1.53–2.23 eV of internal energy in the parent ion, and the two barriers TS4 and TS6 are predicted to be greater in energy, 2.19 and 1.94 eV above the ground state of c-$C_3H_6S^+$. Accordingly, if reactions via TS4 and TS6 are the rate-determining steps and the barriers must be surmounted, then CH_3CS^+ signal is absence in this region.

5. Conclusion

We have investigated the dissociation of energy-selected c-$C_3H_6S^+$ to form $H_2CS^+ + C_2H_4$ in a region 10.2–10.9 eV with a TPEPICO technique. We obtained branching ratios and average releases of kinetic energy for channel c-$C_3H_6S^+ \rightarrow H_2CS^+ + C_2H_4$ from the coincidence mass spectra. Small releases of kinetic energy near the appearance threshold agree with QET calculations with a linearly extrapolated dissociation threshold at 10.39 ± 0.01 eV. This statistical energy distribution is supported by a predicted dissociation mechanism that proceeds without an exit barrier. We discuss plausible dissociation mechanisms for channel c-$C_3H_6S^+ \rightarrow CH_3CS^+ + CH_3$ of the least energy to rationalize the lack of observation of CH_3CS^+ based on G3B3 calculations.

Acknowledgement

We thank the NSRRC and the NSC of Taiwan (Contract No. NSC94-2113-M-213-002) for financial support and the NCHC for providing computing time for calculations.

References

[1] D.M. Turnbull, M.G. Sowa, B.R. Henry, J. Phys. Chem. 100 (1996) 13433.
[2] D.O. Harris, H.W. Harrington, A.C. Luntz, W.D. Gwinn, J. Chem. Phys. 44 (1966) 3467.
[3] D.R. Dice, R.P. Steer, J. Phys. Chem. 77 (1973) 434.
[4] D.R. Dice, R.P. Steer, Can. J. Chem. 53 (1975) 1744.
[5] S. Braslavsky, J. Heicklen, Chem. Rev. 77 (1977) 473.
[6] F.H. Dorer, M.E. Okazaki, K.E. Salomon, J. Phys. Chem. 85 (1981) 2671.
[7] H.A. Wiebe, J. Heicklen, J. Am. Chem. Soc. 92 (1970) 7031.
[8] F. Qi, L. Sheng, M. Ahmed, D.S. Peterka, T. Baer, Chem. Phys. Lett. 357 (2002) 204.
[9] J.J. Butler, T. Baer, Org. Mass Spectrom. 18 (1983) 248.
[10] J.J. Butler, T. Baer, J. Am. Chem. Soc. 104 (1982) 5016.
[11] M.J. Polce, C. Wesdemiotis, Rapid. Commun. Mass Spectrom. 10 (1996) 235.
[12] B. Ruscic, J. Berkowitz, J. Chem. Phys. 98 (1993) 2568.
[13] B.P. Tsai, T. Baer, A.S. Werner, S.F. Lin, J. Phys. Chem. 79 (1975) 570.
[14] H. Shiromaru, Y. Achiba, Y.T. Lee, J. Phys. Chem. 91 (1987) 17.
[15] Y.-S. Fang, I.-F. Lin, Y.-C. Lee, S.-Y. Chiang, J. Chem. Phys. 123 (2005) 054312.
[16] S.-Y. Chiang, C.-I. Ma, J. Phys. Chem. A 104 (2000) 1991.
[17] M.J. Frisch, et al., Gaussian Inc., Pittsburgh, PA, 2003.
[18] P.D. Mollere, K.N. Houk, J. Am. Chem. Soc. 99 (1977) 3226.
[19] R. Stockbauer, Int. J. Mass Spectrom. Ion Phys. 25 (1977) 89.
[20] T. Baer, G.D. Whillett, D. Smith, J.S. Phillips, J. Chem. Phys. 70 (1979) 4076.
[21] C.E. Klots, J. Chem. Phys. 58 (1973) 5364.
[22] C.E. Klots, Adv. Mass Spectrom. 6 (1974) 969.
[23] C.E. Klots, J. Chem. Phys. 64 (1976) 4269.
[24] H.-L. Lee, W.-K. Li, S.-W. Chiu, J. Mol. Struct. (THEOCHEM) 625 (2003) 237.
[25] H.-L. Lee, W.-K. Li, S.-W. Chiu, J. Mol. Struct. (THEOCHEM) 620 (2003) 107.
[26] S.-Y. Chiang, Y.-S. Fang, J. Electron Spectrosc. Relat. Phenom. 144 (2005) 223.